Ecotoxicology and Human Environmental Health

An integrated multilevel analysis profiling biosafety and toxicity induced by Indium- and Cadmium-based quantum dots *in vivo*

Mariateresa Allocca, Lucia Mattera, Antonella Bauduin, Beata Miedziak, María Moros, Luca De Trizio, Angela Tino, Peter Reiss, Alfredo Ambrosone, and Claudia Tortiglione

Environ. Sci. Technol., **Just Accepted Manuscript** • DOI: 10.1021/acs.est.9b00373 • Publication Date (Web): 01 Mar 2019

An integrated multilevel analysis profiling biosafety and toxicity induced by Indium- and Cadmium-based quantum dots *in vivo*

Mariateresa Allocca[1$¶], Lucia Mattera[2#¶], Antonella Bauduin[1], Beata Miedziak[1&], Maria Moros[1§], Luca De Trizio[3], Angela Tino[1], Peter Reiss[2], Alfredo Ambrosone[4], Claudia Tortiglione[1*]*

1 Istituto di Scienze Applicate e Sistemi Intelligenti "E. Caianiello", Consiglio Nazionale delle Ricerche, Via Campi Flegrei, 34 80078 Pozzuoli, Italy

2 Univ. Grenoble-Alpes, CEA, CNRS, INAC-SyMMES, STEP, 38000 Grenoble, France

3 Nanochemistry Department, Istituto Italiano di Tecnologia, Via Morego 30, 16163 Genova, Italy

4 Department of Pharmacy, University of Salerno, Via Giovanni Paolo II 134D, 80084, Fisciano, Italy

Present addresses

$ Istituto di Chimica Biomolecolare, Consiglio Nazionale delle Ricerche, Via Campi Flegrei, 34 80078 Pozzuoli, Italy

Department of Information and Electrical Engineering and Applied Mathematics (DIEM), University of Salerno, Via Giovanni Paolo II 132, 84084 Fisciano, Italy

& University of Rzeszów, Faculty od Biotechnology, Department of Genetics Pigonia Street, 35-310 Rzeszów, Poland

§ Instituto de Ciencia de Materiales de Aragón. Campus Rio Ebro,C/ Mariano Esquillor s/n 50018 Zaragoza (Spain)

.

* corresponding authors: claudia.tortiglione@cnr.it; aambrosone@unisa.it

¶ These authors contributed equally

Abstract

Indium phosphide quantum dots (QDs) have emerged as a new class of fluorescent nanocrystals for manifold applications, from biophotonics to nanomedicine. Recent efforts in improving the photoluminescence quantum yield, the chemical stability and the biocompatibility turned them into a valid alternative to well established Cd-based nanocrystals. *In vitro* studies provided first evidence for the lower toxicity of In-based QDs. Nonetheless, an urgent need exists for further assessment of the potential toxic effects *in vivo*. Here we use the freshwater polyp *Hydra vulgaris*, a well-established model previously adopted to assess the toxicity of CdSe/CdS nanorods and CdTe QDs. A systematic multilevel analysis was carried out *in vivo, ex vivo* and *in vitro* comparing toxicity endpoints of CdSe- and InP-based QDs, passivated by ZnSe/ZnS shells and surface functionalized with penicillamine. Final results demonstrate that both the chemical composition of the QD core (InP *vs.* CdSe) and the shell play a crucial role for final outcomes. Remarkably, in absence of *in vivo* alterations, cell and molecular alterations

revealed hidden toxicity aspects, highlighting the biosafety of InP-based nanocrystals and outlining the importance of integrated multilevel analyses for proper QDs risk assessment.

Table of Contents (TOC)

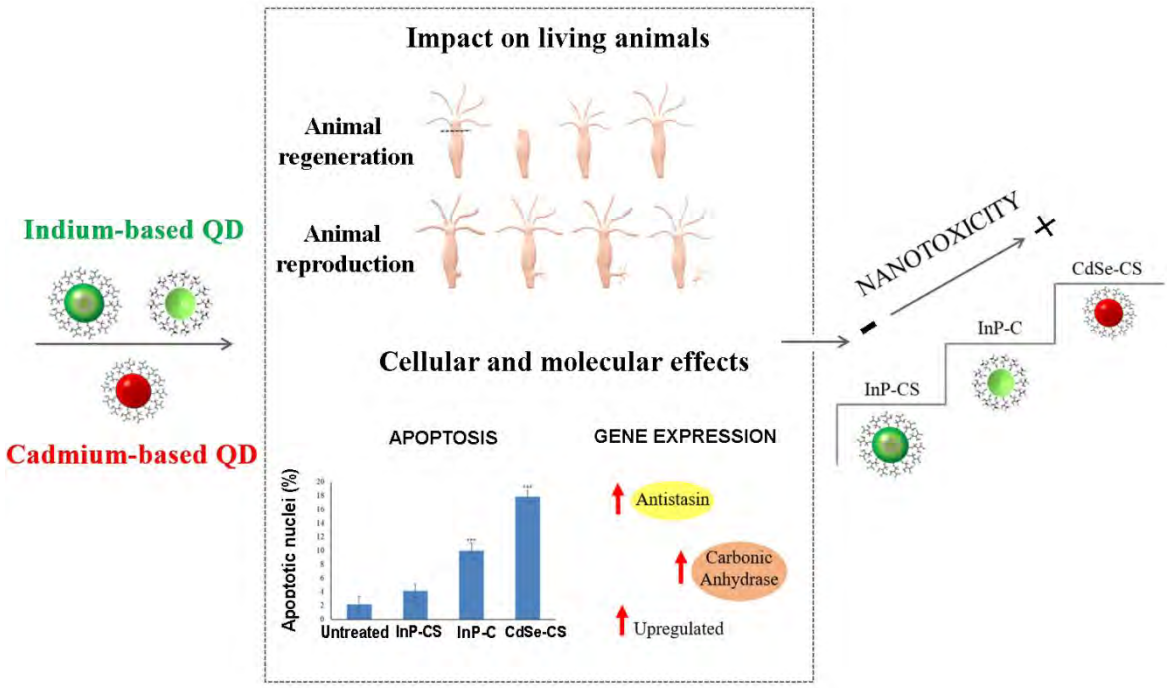

INTRODUCTION

Colloidal semiconductor nanocrystals (NCs), also called quantum dots (QDs), are becoming established fluorophores in many applications, including electronics, biology and medicine.[1] As a consequence the environmental concerns related to QDs synthesis and use are growing up fast. Information about the behaviour, transformation, fate, mode of actions and ecotoxicity of QDs in aquatic environments provide evidences that QDs may threaten the ecosystem at various trophic levels[2], even at very low concentrations (< mg L^{-1} in the case of cadmium-based QDs). In this respect, the most developed systems so far are Cd-based QDs, which are characterized by an excellent photoluminescence quantum yield (PLQY) approaching unity, narrow photoluminescence (PL) line width, and a functionalizable surface, which can be decorated in principle with any type of bioactive molecule.[3, 4] These properties make them very promising tools to address several issues: from targeted drug delivery[5] over multiplexed bioimaging,[6] to monitoring electrical signals in neurons[7]. On the other hand, due to their intrinsic toxicity the

potential of Cd-based QDs for real-life biological imaging and diagnostics applications is very limited and their use *in vivo*, in humans, is obviously precluded, even though environmental issues persist. In light of this, eco-friendly QDs are attracting much attention over the last decade as alternative nanocrystals.[8, 9]

Among the possible semiconductor materials, indium phosphide (InP) NCs were spotted as one of the most promising candidates.[10] Their PL can be tuned from the blue to the near infrared (NIR) region of the spectrum by varying the NC size from around 2 to 6 nm due to the quantum confinement effect. Furthermore, although very limited in number, toxicological studies indicated a much lower intrinsic toxicity as compared to CdSe QDs.[11] While the optical properties of InP QDs in terms of PLQY and line width are inferior to those of CdSe QDs, significant progress in their chemical synthesis has been made in the past decade.[12] A single-step synthesis of InP/ZnS core/shell QDs reaching a PLQY of 30% was initially reported,[13, 14] and further improvements with values exceeding 80% were obtained by growing a thin GaP interfacial layer between the InP core and the ZnS shell or by using Zn(Se,S) graded shells.[15, 16]

Since as-synthesized colloidal core/shell NCs are generally coated with hydrophobic organic surfactants (i.e. long chain carboxylic acids), which make them soluble exclusively in non-polar solvents, their phase transfer to aqueous media is an essential fundamental step for their use in biology. Ligand exchange procedures involving the aminoacid D-penicillamine (Pen) have been recently demonstrated to efficiently work in the aqueous phase transfer of InP-based NCs. Indeed, this small zwitterionic ligand was found to guarantee the colloidal stability of InP/ZnS NCs in a wide range of physiologically relevant pH values, and to promote weak interactions with other biomolecules. [17]Moreover, in contrast to more widely used cysteine (Cys),[18] Pen has a much lower propensity for dimerization under disulphide formation due to two methyl groups in vicinity of the sulfhydryl functions. This has important consequences on both the colloidal stability and PLQY of the phase-transferred QDs, disulphides acting as efficient fluorescence quenchers.[17] Using this approach, stable and strongly luminescent Pen-capped InP QDs could be conjugated with a specific antibody and successfully used as probes in highly sensitive sandwich immunoassays based on Förster resonance energy transfer (FRET).[19, 20] Further examples of

biological applications of Pen-capped InP/ZnS QDs include multimodal imaging probes achieved by grafting Gd-complexes on their surface[21, 22] as well as bi-luminescent probes obtained by sensitizing the emission of grafted Eu or Yb complexes.[23]

In this work, we carry out an exhaustive toxicological evaluation by using an invertebrate model organism, *Hydra vulgaris*. Previously we showed that *Hydra* is an amenable model to test the interaction of several nanomaterials, including QDs, with biological systems.[24-30] This small animal, shaped as a polyp of a few millimetres with jellyfish consistency, has a very simple anatomy, with no organs or biological fluids, but only two layers of epithelial cells surrounding an empty cavity, and a crown of tentacles used for prey capture. When *Hydra vulgaris* is exposed to nanoparticles, by the simple soaking, a behavioural response (such as contractions, elongations, tentacle writhing) or morphological damages (tissue disintegration, swelling) may be elicited immediately, providing first toxicological indications. Going deeper into mechanistic details, fluorescence microscopy can provide information on the uptake mechanism (influenced by membrane interactions), while cell analysis can indicate the induction of apoptosis (by looking at pyknotic nuclei and

membrane integrity). Finally, the molecular analysis by mean of gene expression profiling may help to dissect the involvement of distinct molecular pathways. A comprehensive toxicological analysis was performed in *Hydra* to assess the overall effects of several Cd-based QDs. These studies revealed a high degree of toxicity for aqueous synthesized CdTe QDs,[25, 30,31] while CdSe/CdS nanorods coated with polyethylene glycol (PEG),[32] induced either a behavioural response[33] or an active internalization[28] without signs of morphological damages. The role of the surface charge was also recently investigated and CdS/ZnS QDs coated with a positively charged polymer were found to induce a massive gene deregulation together with evident tissue damages.[24] All these findings depict *Hydra* as a model of choice to analyze how chemical composition, size, surface charge and coating drive QD toxicity.

Here we report a comparative study performed in *Hydra* between Pen-coated InP-based QDs with different shell thicknesses, and we correlate the results with those generated by Pen-coated CdSe/ZnS QDs. The experimental design was conceived not only to test *in vivo* the biocompatibility of the Pen organic coating, but also to directly compare QDs with different core

composition and same coating, and to dissect the contribute of metal components to animal toxicity. Moreover, our study expands the current toxicological knowledge of QDs, which is mainly focused on Cd-based systems, and confirms the higher biosafety of InP-based QDs for biophotonic and nanomedicine applications. Furthermore, it provides potential molecular biomarkers to detect subtle adverse effects also in absence of evident morphological alterations.

Materials and Methods

QDs synthesis and aqueous phase transfer

The detailed experimental procedures are given in Supporting Information. InPZnS QDs ("InP-C") consisting of an InPZnS alloy core and a thin ZnS shell[14] were synthesized following a reported procedure.[13] To increase the shell thickness, an additional, graded Zn(Se,S) shell was grown on the surface of the InPZnS QDs ("InP-CS"), according to the procedure published by Lim *et al.*[34] Hydrophobic CdSe/ZnS QDs ("CdSe-CS") were purchased from Life Technologies/Thermo Fisher Scientific (QD655). All types of QDs were transferred from the organic (chloroform) to the water phase by means

of a biphasic ligand exchange reaction using penicillamine in presence of TCEP at pH 9.[17] Phase transfer is accomplished within 2 h and the aqueous phase is purified by gel chromatography using Sephadex NAP-5™ columns and distilled water for elution.

Inductively Coupled Plasma (ICP) elemental analysis

ICP elemental analysis was carried out via inductively coupled plasma optical emission spectroscopy (ICP-OES) using an iCAP 6300 DUO ICP-OES spectrometer (Thermo Fisher Scientific). All chemical analyses performed were affected by a systematic error of about 5%. 150 polyps were incubated for 24 h with 70 nM dispersion of InP-C, InP-CS or Cd-CS QDs. After extensive washes with Hydra culture medium, the polyps were digested by the addition of concentrated acid (HCl/HNO_3 3:1 (v/v) mixture). The supernatant was diluted using Milli-Q water and analysed, without any further operations. The estimation of the intracellular Indium and Cadmium content was normalized to the number of test animals.

***Hydra* culture**

Hydra vulgaris were cultured in *Hydra* medium comprising 1 mM calcium chloride and 0.1 mM sodium hydrogen carbonate at pH 7.[35] The animals were fed on alternate days with *Artemia* nauplii at 18°C with a 12:12 h light: dark regime. Polyps from homogeneous populations, adult polyps without bud, were selected for the experiments.

Determination of *in vivo* toxicity endpoints

Morphology - Toxicity tests were carried out on groups of 20 polyps, placed into plastic multiwells maintained at a temperature of 18°C. A range of nominal concentrations was selected for InP- and Cd-based QDs, to assess the progressive effects on the morphology and physiology of individual polyps. QD chronic exposure was carried out for 24, 48 and 72 h, refreshing the test solution every 24 h. Effects were monitored and recorded by microscopic examination of each polyp at 24 h intervals. A numerical score, previously introduced by Wilby[36] was used to indicate progressive morphological alterations induced by the toxicant, ranging from 10 to indicate a normal morphology, down to 0 to indicate polyp disintegration. Median score values were determined and used for statistical analysis. TraceCERT

209 standards (Sigma – Aldrich) for Indium and Cadmium were employed as
210 references for ICP.
211
212 Reproduction efficiency **-** Animals (5 *Hydra* with one bud) were treated with
213 70 nM of QDs for 24 h. After QD exposures the animals were washed five
214 times by adding an excess of fresh Hydra medium and kindly pipetting for
215 30 seconds to remove residual nanocrystals, afterward the polyps were
216 placed in 3.5 cm petri dishes (1 *Hydra*/dish). Control polyps at the same
217 developmental stage were not treated. Both treated and untreated *Hydra*
218 were fed daily for 14 days. Population growth rates were determined by
219 considering the growth rate of an exponentially growing group of 5 founder
220 animals as $ln(n/n_0) = kt$ where k is the constant growth, n is the number of
221 animals at time t and n_0 the number of animal at t_0.[37] Three independent
222 experiments were performed.
223 Regeneration efficiency **-** Groups of 20 polyps were incubated in presence of
224 70 nM QDs for 24 h, washed and then bisected in the upper gastric region
225 and allowed to regenerate in fresh medium. The regenerating heads were
226 classified as stage 0 (wound closure), stage 1 (tentacle bud) and stage 2

(tentacle length reaching ¼ of final length). Developmental stages were monitored through a stereomicroscope every 24 h and relative percentages estimated at each time point for all QD conditions compared to untreated polyps.

***In vitro* toxicity endpoints**

Assessment of apoptosis - Apoptotic cell rate was evaluated by 4'-6-Diamidino-2-phenylindole (DAPI) nuclear staining. Both QD-treated (50 nM, 24 h incubation) and untreated polyps were macerated into single cell suspensions, using a solution composed of acetic acid, glycerol and H_2O in a 1:1:13 (v/v) ratio.[38] Dissociated cells were fixed with 4% paraformaldehyde and spread on slides, then washed with PBS (NaCl 137 mM, KCl 2.7 mM, Na_2HPO_4 10 mM, KH_2PO_4 1.8 mM) and finally stained with DAPI for 2 min. Two independent cell macerations were analysed and more than 300 cells were counted for each treatment in order to determine the percentage of apoptotic nuclei. Imaging was performed using an inverted microscope (Axiovert 100, Zeiss, MA, USA) equipped with a digital colour camera (Olympus, DP70).

The software system Cell F (Olympus) was used for imaging acquisition and analysis.

Gene expression analysis - Differences in gene expression profiles induced by QD treatment were assessed by quantitative real time polymerase chain reaction (qRT-PCR). For each experimental condition, RNA was extracted from groups of 25 animals by purification in Trizol Reagent (Life Technologies) according to the manufacturer's instructions. RNA was quantified and quality checked by SmartSpec plus spectrophotometer (Biorad, CA, USA) and agarose gel electrophoresis, respectively. RNA samples were treated with DNaseI *(Amplification Grade, Invitrogen)* according to supplier's instructions. The first-strand cDNA was synthesized by High Capacity cDNA Reverse Transcription Kit (Applied Biosystem) using 0.5 µg of DNA-free RNA in a final volume of 10 µL. qRT-PCR was performed in 25 µL of reaction mixture consisting of 1x Express SybrR GreenER qPCR SuperMix with premixed ROX (Invitrogen), serial cDNA dilutions and 0.3 µM each primer. The reactions were processed using the StepOne Real-Time PCR System (Applied Biosystem) according to the following thermal profile: 95°C for 2 min, one cycle for cDNA denaturation; 95°C for 15 sec and 60°C for 1 min,

40 cycles for amplification. Specific primers of *Hydra* homologues genes of antistasin *(XM_002158823),* and carbonic anhydrase *(XM_002154950.1)* were designed using Primer3 software (http://frodo.wi.mit.edu/primer3/) and are listed in table S1. Gene expression was evaluated in QD treated and untreated polyps; three technical replicates from three independent experiments were carried out. The expression profiles were analysed by applying the ΔΔCt method[39] where the values of the gene of interest were normalized for the values of reference control gene *Hydra Elongation Factor 1α* (Z68181.1*).*

RESULTS AND DISCUSSION

Two types of InP-based QDs differing in their passivating zinc chalcogenide shell were synthesized in order to test their colloidal stability in aqueous solutions and overall behaviour during *in vivo* experiments: alloyed InPZnS QDs containing a thin ZnS shell (termed "InP-C") prepared in a single-step one-pot reaction[13] and InPZnS/ZnSe/ZnS QDs (termed "InP-CS") obtained by growing an additional $Zn(Se_{0.1}S_{0.9})$ gradient shell on the surface of the latter. The phase transfer of both types of samples to water was achieved by

279 ligand exchange, mixing a dispersion of QDs in chloroform and an aqueous
280 solution at pH 9 containing penicillamine (Pen), in presence of the mild
281 reducing agent TCEP (tris-(2-carboxyethyl)-phosphine (see also SI). Basic pH
282 promotes the deprotonation of the thiol group of Pen, which results in
283 stronger binding to the surface of the different ZnS-coated QDs. On the
284 other hand, the reducing agent TCEP prevents the formation of penicillamine
285 disulfide which may reduce the colloidal stability and the PLQY of the final
286 systems.[17] Commercial CdSe/ZnS core/shell QDs (CdSe-CS) were
287 functionalized with Pen using the same approach. Structure, net-charge and
288 optical properties of the different QDs are shown in Figure 1, SI Figure S1,
289 S2 and Table S2. The sizes of QDs measured in Hydra medium were 9 nm,
290 6.6 and 7.6 nm for CdSe-CS, InP-C and InP-CS, respectively. Slight or no
291 modifications were observed among the mean diameters measured in water
292 (Figure S1), suggesting that the testing medium does not promote QD
293 aggregation and/or precipitation.

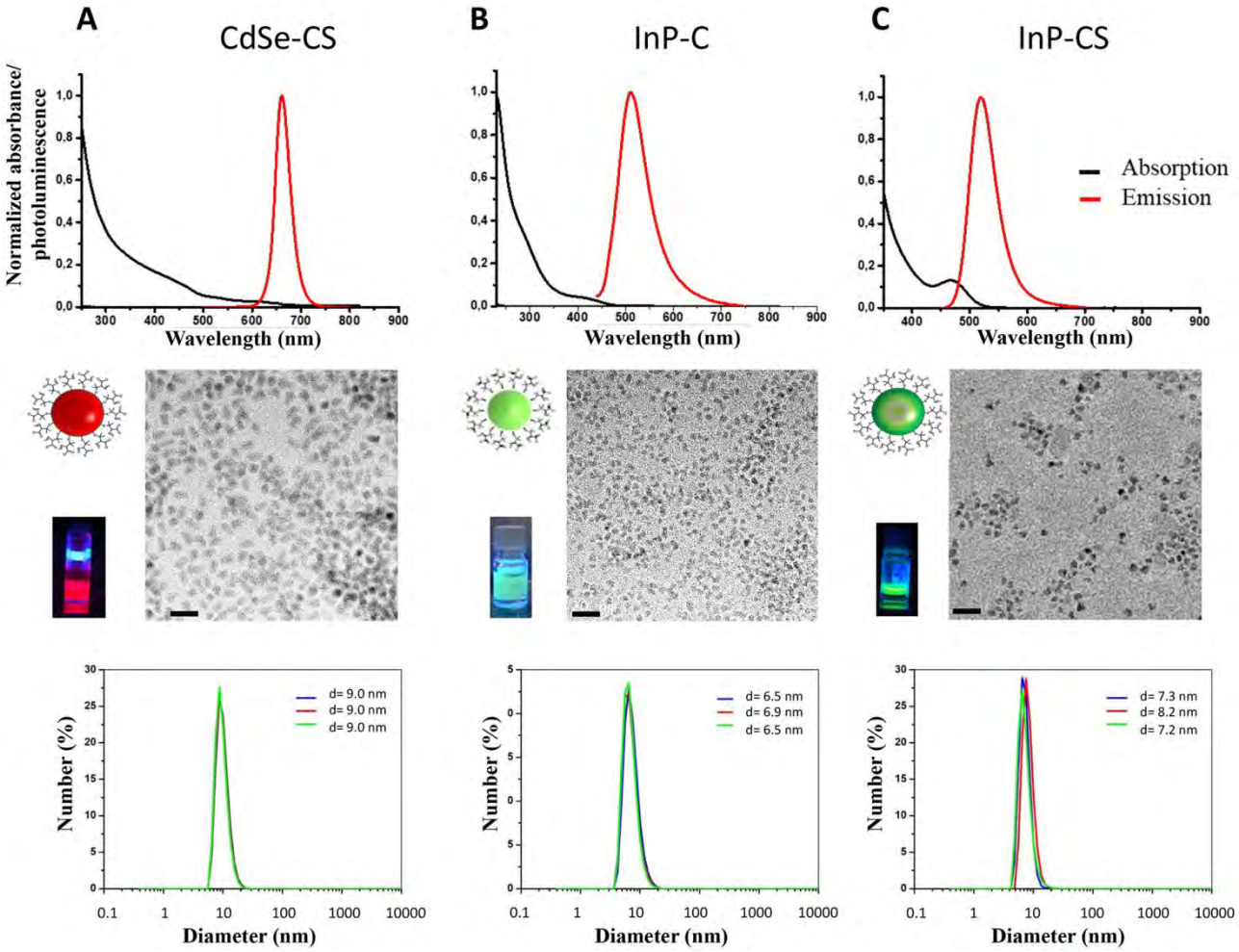

294

295 **Figure 1**. Physical characterization of QDs. Optical properties (upper panel),

296 schematic structure and TEM images (middle panel) and DLS measurements

297 in *Hydra* medium (lower panel) of the different types of QDs: A) CdSe-CS B)

298 InP-C and C) InP-CS. The UV-Vis (black line) and PL (red line) spectra of

299 the QDs have been taken after aqueous phase transfer with penicillamine.

300 Scale bar: 50 nm in all images.

301

Considering that these nanocrystals present similar physico-chemical features (size, shape, charge and coating), we evaluated their biological impact by normalising their toxicity on QD concentration. To study the interactions of QDs with *Hydra*, living polyps were exposed to different concentrations of QDs (from 25 nM to 100 nM) in their culture medium. This range of concentration was selected on the basis of our previous works carried out with different types of nanocrystals [24-27, 30].

After 24 h the animals were thoroughly rinsed to remove QDs that adhere to the external epithelium and inspected by fluorescence microscopy. InP-C treated animals did not show any fluorescence, which suggests that QDs have either a PLQY too low for detection (SI Figure S2 and Table S2) and/or that PL quenching occurred during their internalization/incubation period.

On the other hand, polyps incubated with InP-CS and CdSe-CS (at a concentration of at least 50 nM) showed fluorescent foci uniformly dispersed throughout the whole animal body, as reported in Figure 2. This labelling pattern reflects the QDs accumulation into intracellular granular-like storage structures, and it may depend on macropynocitosis, i.e. the internalization of

320 a large fraction of external fluids, as observed in our previous works.[28, 40]
321 The fluorescence staining appeared clear and much stronger in CdSe-CS
322 treated animals, and this might be due to a difference in their uptake
323 efficiency, in their PLQYs, or/and photostability within *Hydra* tissues.
324 In *Hydra*, as in other eukaryotic systems, the net surface charge of
325 nanomaterials influences the uptake efficiency, and the positive charge
326 greatly enhances the internalization rate because of the electrostatic
327 interaction with the negatively charged biological membranes.[28] Herein, we
328 observed that negatively charged QDs (as reported in SI Table S2) were
329 also taken up by *Hydra* polyps, although at a minor extent.
330

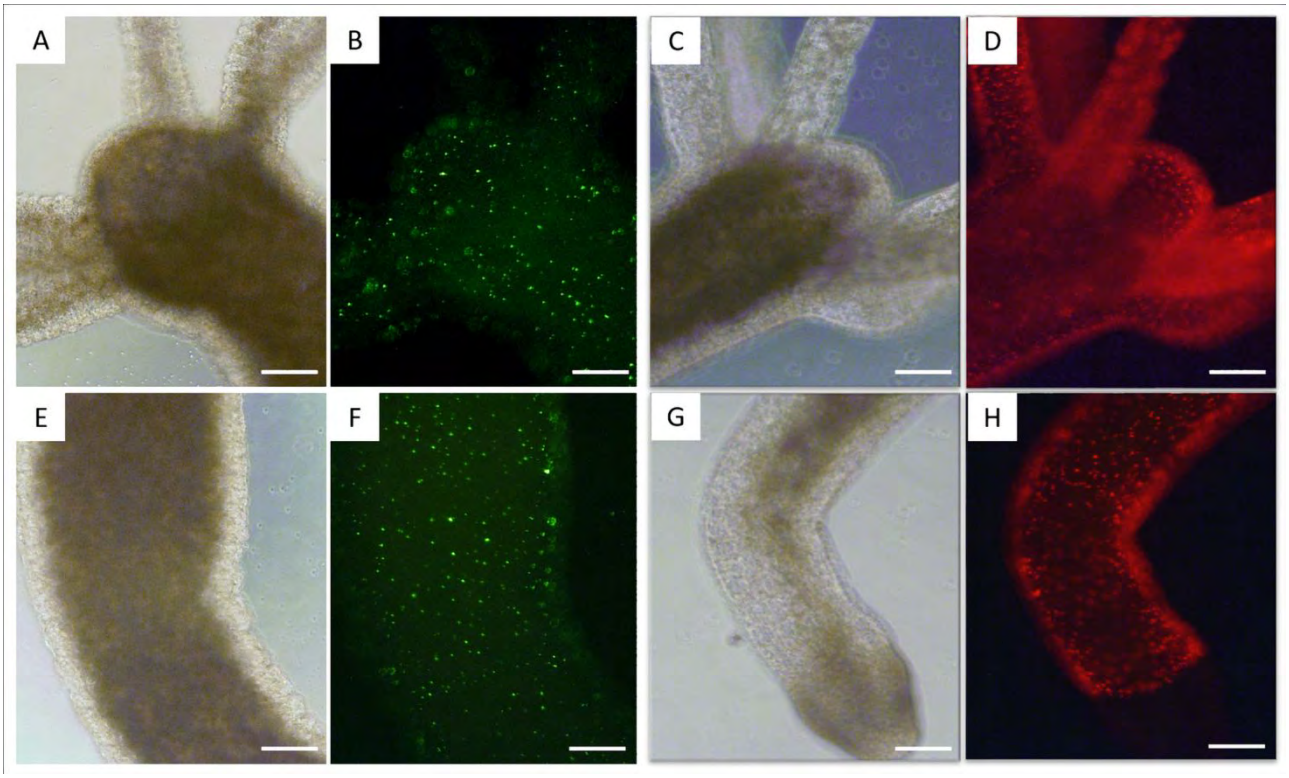

Figure 2. Biodistribution of InP- and CdSe-based QDs in *Hydra*. Bright-field and fluorescence images of *Hydra* treated with InP-CS QDs (two left columns) and CdSe -CS QDs (two right columns). A spotted fluorescence pattern is uniformly distributed from head (B, D) to foot regions (F, H) of treated animals. A, C, E, G show the corresponding images in bright field. Scale bar: 200 μm.

Due to the intrinsic lower fluorescence of the InP QDs, to investigate whether or not the fluorescence difference was due to differences in the uptake efficiency, elemental analyses by mean of ICP were conducted on

large number of polyps (around 150) treated with each QD type (70 nM, 24 h). Results showed a greater Indium content for InP-C treated animals compared to InP-CS treatment (47,2 ng of In/Hydra and 17,7 ng of In/Hydra, respectively) indicating that the lower photoluminesce of InP-C compared to InP-CS is responsible for the absence of fluorescence in InP-C treated polyps, rather than a low rate of internalization. For CdSe-CS QD treated polyps Cadmium content equal to 30,4 ng/Hydra was detected, which is in the same range of the two others.

In vivo evaluation of QD toxicity endpoints

The high sensitivity to heavy metals makes *Hydra* an amenable tool for assessment of inorganic nanoparticle's toxicity in natural ecosystems, modelling biological barriers for their absorption, distribution, and persistency in the food chain. Potential adverse effect of QDs here synthesised were investigated by soaking living *Hydra* polyps with increasing doses of InP-C, InP-CS and CdSe-CS QDs (from 25 nM to 100 nM) and inspected after 24, 48 and 72 h of incubation. Morphological alterations were quantified by using

a methodology assigning numerical values to morphological damages,[25, 36, 41] and visually displayed in Figure 3A and SI Table S3. Median scores recorded at each QD test concentration (Figure 3B) indicate that In based QDs are characterized by a "safer" profile (higher numerical values) with respect to Cd based QDs. Polyps exposed to InP-CS QDs exhibited negligible morphological alterations even at the highest test concentration (100 nM), while InP-C revealed a substantial safe profile up to 50 nM. Conversely, animals exposed to CdSe-CS displayed evident morphological changes, leading to death at 72 h time point (Figure 3B). These data are in line with our previous works on cadmium telluride (CdTe) QDs,[25] demonstrating high toxicity of Cd-based QDs, independently from the organic coating.[24, 42] Conversely, In-based QDs produce reversible effects, similar to those reported for non-toxic nanomaterials (e.g. carbon nano-onions and silica NPs) tested in *Hydra* at same doses (50-100 nM).[26, 27] Comparison of InP-C and InP-CS QDs effects on *Hydra* morphology demonstrates that the inorganic zinc chalcogenide shell attenuates the Indium effect. On the other hand, it does not counteract CdSe-CS QDs toxicity, suggesting either partial degradation in animal tissues or leaking of free heavy metals out the inner

core. This also indicates that the toxicity of the QDs is mainly driven by the core components.

Next, the modulations of two important physiological processes were chosen as additional endpoints, *i.e.* the reproduction and regeneration efficiencies, known to be harshly impaired by chemical pollutants. For both experiments, we exposed the animals to 70 nM QDs. This intermediate dose was selected according to the outcomes obtained by the morphological analyses (Figure 3B), showing that concentrations higher than 50 nM (for InP QDs) and lower than 100 nM (for CdSe QDs) may ensure induction of a robust, but not lethal effect for both QD types

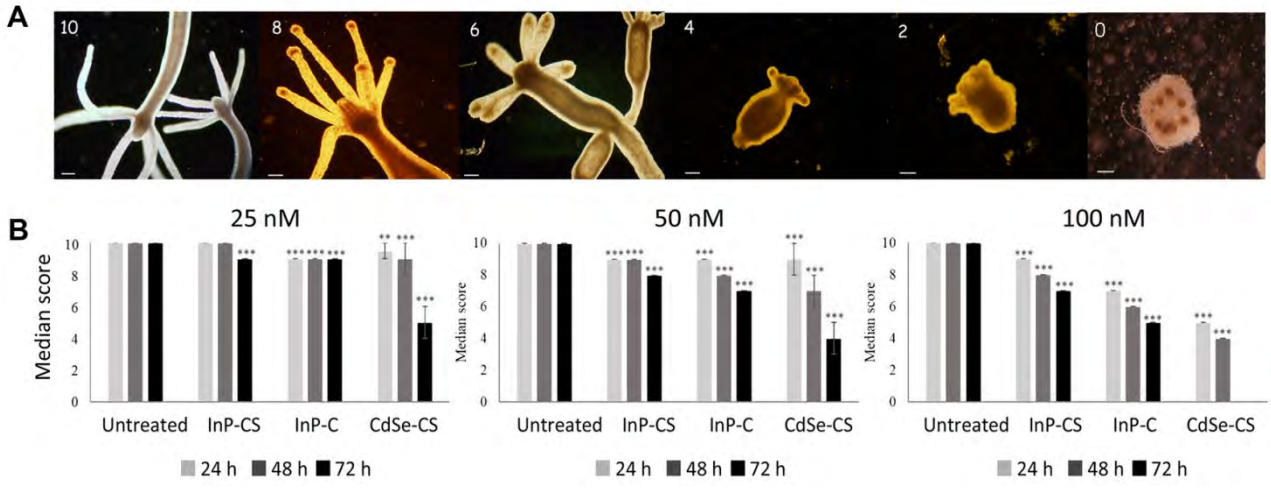

Figure 3. Morphological changes and associated numerical score system employed for toxicological analysis. A) *Hydra* polyps respond to

391 environmental stimuli and nano-insults through a broad range of
392 morphological changes, which range from tentacle contractions, then body
393 contraction and swelling, up to tentacle loss and whole tissue disintegration.
394 These morphological phenotypes are quantified on a large number of animals
395 by associating each phenotype to a numerical score, ranging from 10
396 (healthy animal) to zero (animal death). B) Dose-responses histograms of
397 *Hydra* polyps exposed to different QDs. The median score value is reported
398 for each QD type, QD concentration and treatment duration. Three
399 independent experiments were carried out. Asterisks denote significant
400 difference between untreated and treated polyps (*, $P< 0.05$; **, $P< 0.01$,
401 ***, $P< 0.005$) according to a post-hoc Mann Whitney U Test. Scale bars,
402 100 μm

403

404 Owing to the superb plasticity of the *Hydra* cells and tissues, adult polyps
405 can regenerate body parts after amputation and restore morphogenetic
406 processes. Normally these processes start a few minutes post amputation
407 and culminate in the formation of the missing parts of the body, namely the
408 head or the foot in three/four days. Any stress applied during this period

409 may result in abnormal regeneration or may slow down and even arrest the
410 process. In this work, healthy polyps were bisected in the upper gastric
411 region and allowed to regenerate (Figure 4A) in presence of 70 nM QDs or
412 in the normal medium. Animal stumps were daily inspected for viability, and
413 regeneration stages were recorded 24, 48 and 72 h post amputation. Stage
414 0 indicates a complete inhibition of regeneration (0 tentacle), stage 1
415 indicates heads with emerging tentacle (one or two), while stage 2 denotes a
416 normal regeneration (tentacle length reaching ¼ of final length). Polyp
417 exposure to InP-CS QDs slightly impaired the regeneration patterning during
418 the first 48 h, as shown by the lower percentage (40%) of polyps present in
419 stage 2 compared to untreated polyps (60%). This inhibitory effect was totally
420 transient as at 72 h the polyps paralleled untreated animals. A similar
421 behavior was induced by InP-C QDs, while CdSe-CS QDs caused complete
422 inhibition of regeneration in 80% of treated animals and this effect could not
423 be recovered (60% of polyps still in stage 0 and stage 1 at 72 h).
424

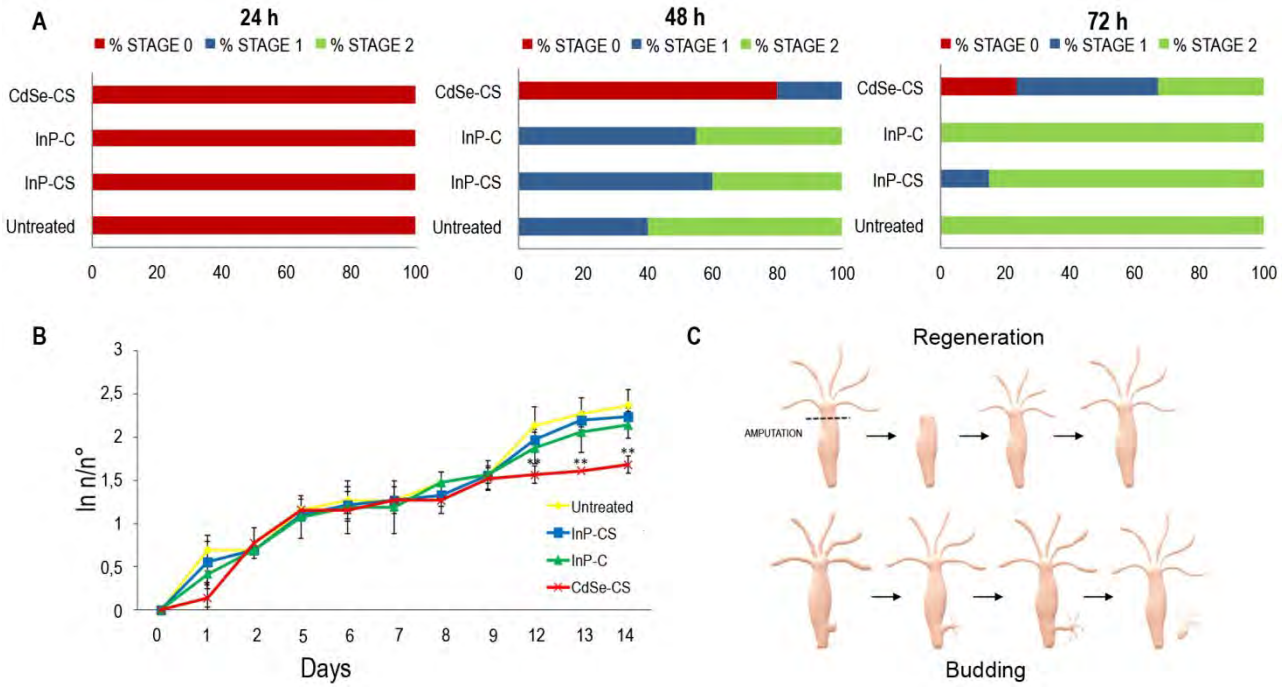

425

426 **Figure 4.** Influence of InP-based QDs on *Hydra* regeneration and

427 reproduction. A) Impact of QDs (70 nM) on regeneration. The regenerating

428 polyps were observed through a stereomicroscope and grouped in three

429 stages according to their developmental stage. Histograms are representative

430 of a single experiment. Three independent experiments were carried out. B)

431 Impact of the QDs on reproduction. Five animals with one bud were treated

432 with 70 nM InP-C and InP-CS QDs for 24 h and the following day each

433 animal was washed and placed in a well to monitor progeny. Asterisks

434 denote a significant difference between untreated and CdSe-CS treated

435 polyps (**, $P < 0.01$) according to ANOVA test. C) Schematic representation

436 of *Hydra* regeneration (upper panel) and budding (lower panel) processes.

437

438 We also estimated the reproductive capability of QDs treated polyps. *Hydra*
439 reproduces asexually by budding (schematically represented in Figure 4C),
440 which is sustained by continuous cell proliferation and migration. This
441 process takes approximately 3 days[37]. Environmental factors, such as the
442 presence of aquatic pollutants or the feeding regime may affect significantly
443 cell viability and tissue growth and in turn compromise the normal bud
444 growth and detachment.
445 Thus, the population growth rate is an excellent index to monitor the
446 transgenerational response of *Hydra* to environmental threats. Five polyps
447 (founders) were exposed to 70 nM for 24 h, then extensively washed and
448 allow to originate five independent *Hydra* populations over 14 days. The
449 growth curve shown in Figure 4B indicate a slight delay of the reproduction
450 rate induced by CdSe-CS QDs but not by InP QDs exposure, showing long
451 term effects of Cd-based QD.

452

453 ***In vitro* assessment of QD toxicity**

454 QDs can negatively affect cell proliferation, differentiation and viability.
455 Moreover, the exposure of cells to QDs may trigger distinct cell death
456 mechanisms. While necrosis often occurs as a result of the direct injury of
457 the cell structure, apoptosis is a programmed cell death, finely concerted by
458 endogenous players. Cells dying by apoptosis undergo evident morphological
459 changes, *i.e.* collapses of the cytoskeleton, disassembling of the nuclear
460 envelop, condensation of chromatin (pyknotic nuclei) followed by breaking up
461 into fragments forming so-called apoptotic bodies. In multicellular organisms,
462 apoptosis occurs physiologically during the growth, development, and
463 maintenance of multicellular organisms and in response to environmental
464 stressors.[43] In *Hydra*, apoptosis regulates many physiological processes such
465 as the oogenesis and spermatogenesis, starvation, and head regenerating
466 tips.[44,45] We recently demonstrated that the programmed cell death may
467 occur in *Hydra* as a defence mechanism in the presence of sub-lethal
468 concentrations of nanomaterials, even in the absence of detectable

morphological alterations, demonstrating the interest of this type of evaluation in case of QD exposure.[25, 26, 46]

To this aim *Hydra* were incubated with 50 nM QD solutions for 24 h, then macerated into fixed single cell suspensions[38] and inspected by fluorescent microscopy. Typically, condensed chromatin forms pyknotic nuclei, which are phagocytised by both the ectodermal and the endodermal epithelial cells.[47, 48] These structures are easily distinguishable by fluorescence microscopy upon 40-6-Diamidino-2-phenylindole (DAPI) staining (Figure 5A). Counts of pyknotic nuclei reported in Figure 5B show that CdSe-CS QDs dramatically increase the apoptotic rate (18%); milder effects were induced by the exposure to In-C QDs even though the apoptotic cell number was significantly higher (10%) compared to untreated animals. Conversely, the InP-CS QDs solution had marginal effects with a percentage of damaged nuclei only slightly higher than control animals, which as mentioned above, normally show a physiological rate of apoptosis. These data confirm a safe profile of InPZnS/(ZnSe,S) QDs in *Hydra,* highlighting two important aspects: the protective role of the shell in reducing the effect of InP-based QDs, and the high toxicity of Cd-based QDs, even protected by the same inorganic shell.

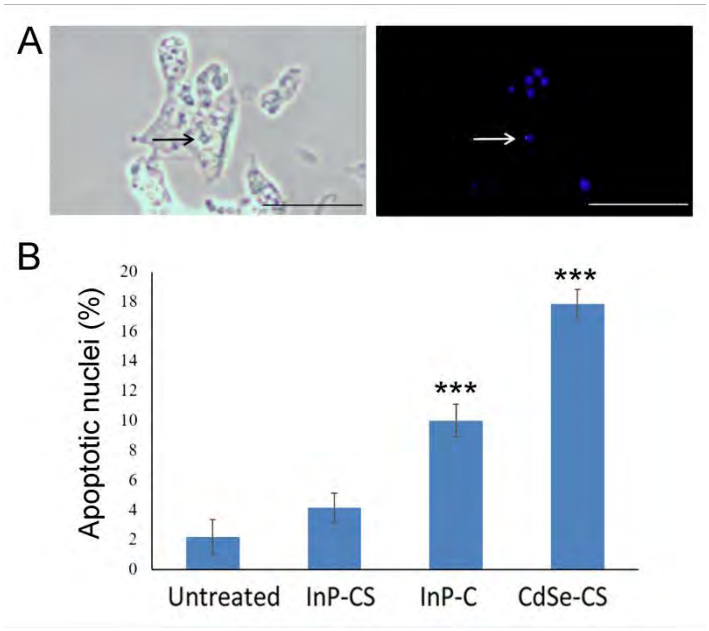

Figure 5. Effect of QDs on *Hydra* apoptotic rate. A**)** Microscope image of single cells prepared from QD treated *Hydra*. Left, an ectodermal epithelial cell in bright field. Right, fluorescence imaging following DAPI staining shows a pyknotic nucleus (white arrow), typical apoptosis hallmark in the epithelial cell. Scale bars: 20 μm. B**)** Quantitative assessment of apoptosis induction. Following 24 h incubation with 50 nM QDs, polyps were macerated in single cells and the percentage of apoptotic cells was determined by counting the DAPI-stained fragmented nuclei. Asterisks

499 denote a significant difference between untreated and QD- treated polyps
500 (***, P< 0.05) according to one-way ANOVA test.
501
502
503 ***Genotoxic effects***
504 Over the last decade, nanotoxicology approaches explored the impact of
505 novel nanomaterials at the molecular level with the aim to unravel genome,
506 epigenome, transcriptome and proteome changes in response to
507 nanostressors.[49] *Hydra* genome sequencing disclosed genetic features finely
508 conserved across Metazoan evolution.[50] Very recently, the conservation of the
509 key regulatory genetic pathways in *Hydra* allowed us to dissect *Hydra*
510 transcriptome modulation in response to different nanomaterials and identify
511 nanotoxicity inducible genes. More precisely, we proved by RNAseq analyses
512 that silica nanoparticles, with a safe profile on animal tests, produced only
513 minor modifications on the gene expression landscape.[27] Conversely,
514 transcriptome profiling of *Hydra* polyps exposed to CdSe/ZnS QDs revealed
515 that the expression of hundreds of genes was radically affected. In particular,
516 two highly overexpressed genes, namely carbonic anhydrase and the serine

517 protease inhibitor antistasin, showed an impressive up-regulation upon 8 h
518 and 24 h QD exposure and might therefore be considered gene signatures
519 of heavy metal-based QDs exposure in *Hydra*. The exploitation of biomarkers
520 based on gene expression is a well-established methodology to provide
521 reliable outcomes about the early molecular response evoked by an
522 exogenous stimulus.[51] *Hydra* polyps were incubated with 50 nM and 100 nM
523 of InP-CS and InP-C QDs and with 50 nM CdSe-CS QDs, for 8 h and 24 h
524 and the biomarker expression was investigated by qRT-PCR (Figure 6). Two
525 distinct concentrations of QD were investigated in order to profile the dose -
526 response fluctuations of biomarkers. In the case of CdSe-CS QDs, we did
527 not test the concentration 100 nM due to the significant presence of necrotic
528 cells. Overall, QD treatments up-regulate the expression of both genes. The
529 highest activation of carbonic anhydrase expression (fold change >25) was
530 detected at 8 h by 100 nM InP-C together with robust overexpression of
531 antistasin at 8 and 24 h (fold change >18). As expected, significant up-
532 regulation of these biomarkers was induced also by CdSe-CS, especially at
533 24 h. Surprisingly, a robust increase of biomarker expression was induced by
534 InP-CS QDs, which is in contrast with the low effect caused on morphology

and biological processes. We suggest that carbonic anhydrase and antistasin may be symptomatic of a more general pollutant exposure, and show the possibility to use them as excellent and sensitive biomarkers of exposure able to probe aquatic pollutants, even at very low concentrations. Further experiments will clarify their use to predict possible harmful effects on animals, which are very difficult to be estimated, as several biological responses are measurable only after protracted exposure.

The functional role of these genes as biomarker for nanotoxicity needs to be established. Antistasin is a 17kDa serine protease inhibitor originally isolated from the salivary glands of the Mexican leech (*Haemanteria officinalis*). It has been shown to be a potent anticoagulant activity and to prevent metastases.[52] Antistasin-like gene is strongly expressed in gland and mucous cells and may be involved in protecting gastric tissues from autodigestion.[53] Although functional studies are demanded, the up-regulation of the protease inhibitor antistasin may represent an attempt to prevent protein degradation likely activated by nanoparticle exposure in *Hydra*. This protective role may also explain the gradual increase of antistasin gene expression observed after a 24 h QD exposure compared to 8 h incubation.

553 Carbonic anhydrase (CA) is a zinc-containing metallo-enzyme, which
554 catalyzes the reversible hydration of carbon dioxide. It contributes to fixation
555 of atmospheric CO_2 and participates in many other physiological processes
556 such as pH homeostasis, electrolyte transport and many biosynthetic
557 reactions.[54] The role of CA as environmental biomarker has been
558 investigated over the recent years.[55] [56] Many works demonstrated that heavy-
559 metal exposure may inhibit CA activity possibly through their capability to
560 bind and displace the native cofactor, producing non-functional CA
561 metallovariants in several species. Conversely, enhanced activity of CA has
562 been described as well in *Chlamydomonas reinhardtii* [57], *Thalassiosira*
563 *weissflogii,* [58] [59] indicating that alternative cofactors (e.g. cadmium) may
564 successfully substitute Zn^{2+} without impairing the catalytic activity. Despite the
565 wealth of data on CA activity, little is known about gene expression
566 modulation in response to chemical pollutants. Although its biological role as
567 biomarker needs to be further elucidated, higher overexpression after 8 h
568 with respect to 24 h treatment suggests that CA may find application as
569 early expression biomarker of nanotoxicity.
570

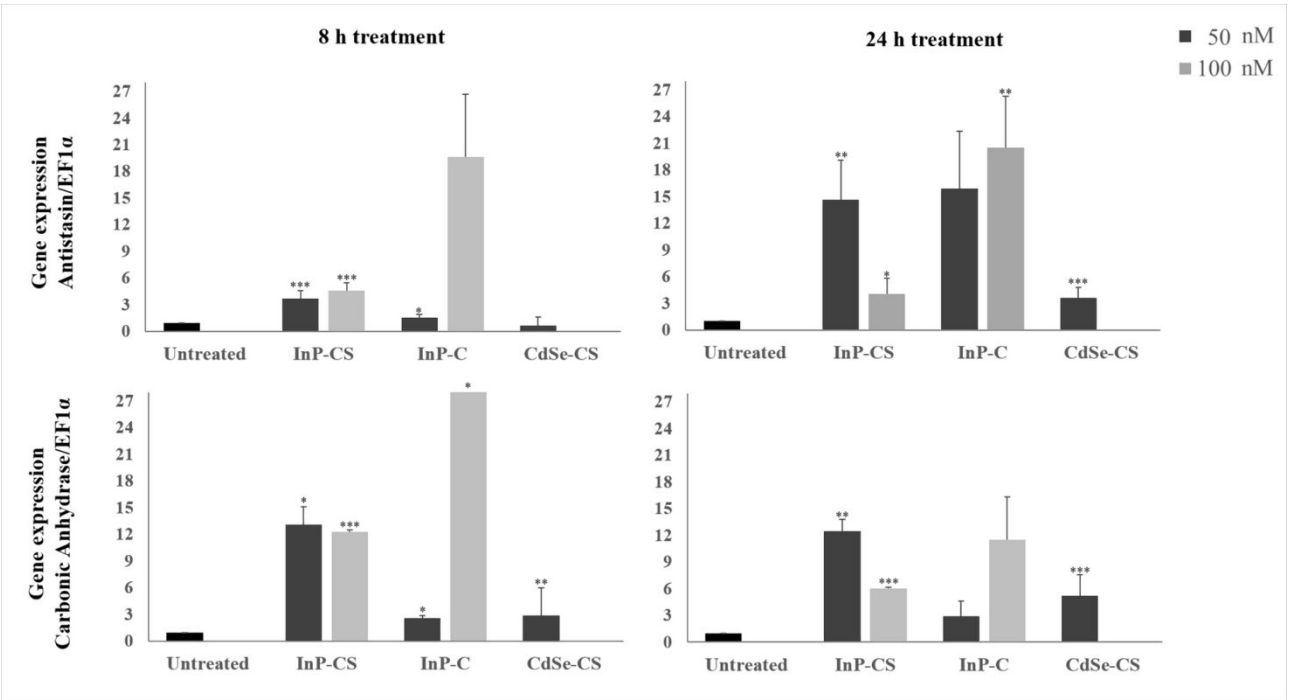

571

572 **Figure 6.** Gene expression profiles of selected stress responsive genes in

573 QDs-treated polyps analyzed by qRT-PCR. The Elongation factor 1-alpha

574 (EF-1α) was used as reference gene. The data represent mean of three

575 biological replicates. The value of each biological replicate is the average of

576 three technical repeats.

577

578 Taken together, our findings suggest that the choice of InP-based QDs

579 appears to be a valid alternative to CdSe-based QDs for manifold

580 applications. Since aquatic species, including freshwater invertebrates, are

581 natural targets for nanoparticles, which possibly contaminate natural waters

582 through sewage effluent and landfill leakages, our results suggest a safety

583 profile of Pen-capped InPZnS/Zn(Se,S) QDs in aquatic organisms, at least at
584 the tested doses. Therefore, considering that *Hydra* is very susceptible to
585 aquatic pollutants, these QDs may not represent a concrete risk for
586 environmental health. Our extensive assessment of toxicity endpoints and
587 comparative analyses may drive future research on other types of eco-
588 friendly Cd-free QDs to monitor aquatic environments, preventing endogenous
589 species health, or estimating bioaccumulation of heavy metals in the food
590 chain up to humans.

591

592

593 **Acknowledgements**

594 L.M. and P.R. acknowledge the French National Research Agency ANR
595 (contracts NANOFRET, ANR-12-NANO-0007-03, NEUTRINOS, ANR-16-CE09-
596 0015-03 and FLUO, ANR-18-CE09-0039-01). We thank Dr. Tim Senden, Dr.
597 Christophe Lincheneau and Dr. Karl David Wegner for QD synthesis and
598 Fabio Agnese for TEM imaging. M.M. acknowledges financial support from
599 the European Union´s Horizon 2020 research and innovation programme
600 (Marie Skłodowska-Curie grant agreement No. 660228).

Supporting Information. S1: Synthesis of InPZnS alloy nanocrystals. S2: Surface modification of QDs with Pen, S-3. Characterization of the QDs. Table S1: Primer sequences used in qRT-PCR analyses. Table S2: Hydrodynamic diameter, zeta-potential and QY values of the used In-and Cd-based QDs. Table S3. Morphological changes and associated scores for toxicological assessment in *Hydra.*

References

1. Zhou, J.; Yang, Y.; Zhang, C.-y., Toward Biocompatible Semiconductor Quantum Dots: From Biosynthesis and Bioconjugation to Biomedical Application. *Chem. Rev.* **2015,** *115*, (21), 11669-11717.

2. Rocha, T. L.; Mestre, N. C.; Saboia-Morais, S. M.; Bebianno, M. J., Environmental behaviour and ecotoxicity of quantum dots at various trophic levels: A review. *Environment international* **2017,** *98*, 1-17.

3. Medintz, I. L.; Uyeda, H. T.; Goldman, E. R.; Mattoussi, H., Quantum dot bioconjugates for imaging, labelling and sensing. *Nat Mater* **2005,** *4*, (6), 435-446.

4. Gill, R.; Zayats, M.; Willner, I., Semiconductor Quantum Dots for Bioanalysis. *Angew. Chem. Int. Ed.* **2008,** *47*, (40), 7602-7625.

5. Zrazhevskiy, P.; Sena, M.; Gao, X. H., Designing multifunctional quantum dots for bioimaging, detection, and drug delivery. *Chem. Soc. Rev.* **2010,** *39*, (11), 4326-4354.

6. Wegner, K. D.; Hildebrandt, N., Quantum dots: bright and versatile in vitro and in vivo fluorescence imaging biosensors. *Chem. Soc. Rev.* **2015,** *44*, (14), 4792-4834.

7. Efros, A. L.; Delehanty, J. B.; Huston, A. L.; Medintz, I. L.; Barbic, M.; Harris, T. D., Evaluating the potential of using quantum dots for monitoring electrical signals in neurons. *Nat Nanotechnol* **2018,** *13*, (4), 278-288.

8. Xu, G.; Zeng, S.; Zhang, B.; Swihart, M. T.; Yong, K. T.; Prasad, P. N., New Generation Cadmium-Free Quantum Dots for Biophotonics and Nanomedicine. *Chemical reviews* **2016,** *116*, (19), 12234-12327.

9. Reiss, P.; Carrière, M.; Lincheneau, C.; Vaure, L.; Tamang, S., Synthesis of Semiconductor Nanocrystals, Focusing on Nontoxic and Earth-Abundant Materials. *Chem. Rev.* **2016,** *116*, (18), 10731-10819.

10. Mushonga, P.; Onani, M. O.; Madiehe, A. M.; Meyer, M., Indium Phosphide-Based Semiconductor Nanocrystals and Their Applications. *J. Nanomater.* **2012**, 869284.

11. Brunetti, V.; Chibli, H.; Fiammengo, R.; Galeone, A.; Malvindi, M. A.; Vecchio, G.; Cingolani, R.; Nadeau, J. L.; Pompa, P. P., InP/ZnS as a safer alternative to CdSe/ZnS core/shell quantum dots: in vitro and in vivo toxicity assessment. *Nanoscale* **2013,** *5*, (1), 307-317.

12. Tamang, S.; Lincheneau, C.; Hermans, Y.; Jeong, S.; Reiss, P., Chemistry of InP Nanocrystal Syntheses. *Chem. Mater.* **2016,** *28*, (8), 2491-2506.

13. Li, L.; Reiss, P., One-pot synthesis of highly luminescent InP/ZnS nanocrystals without precursor injection. *J Am Chem Soc* **2008,** *130*, (35), 11588-+.

14. Huang, K.; Demadrille, R.; Silly, M. G.; Sirotti, F.; Reiss, P.; Renault, O., Internal structure of InP/ZnS nanocrystals unraveled by high-resolution soft X-ray photoelectron spectroscopy. *ACS nano* **2010,** *4*, (8), 4799-805.

15. Kim, S.; Kim, T.; Kang, M.; Kwak, S. K.; Yoo, T. W.; Park, L. S.; Yang, I.; Hwang, S.; Lee, J. E.; Kim, S. K.; Kim, S. W., Highly Luminescent InP/GaP/ZnS Nanocrystals and Their Application to White Light-Emitting Diodes. *J Am Chem Soc* **2012,** *134*, (8), 3804-3809.

16. Lim, J.; Park, M.; Bae, W. K.; Lee, D.; Lee, S.; Lee, C.; Char, K., Highly Efficient Cadmium-Free Quantum Dot Light-Emitting Diodes Enabled by the Direct Formation of Excitons within InP@ZnSeS Quantum Dots. *ACS Nano* **2013,** *7*, (10), 9019-9026.

17. Tamang, S.; Beaune, G.; Texier, I.; Reiss, P., Aqueous Phase Transfer of InP/ZnS Nanocrystals Conserving Fluorescence and High Colloidal Stability. *ACS Nano* **2011,** *5*, (12), 9392-9402.

18. Liu, W.; Choi, H. S.; Zimmer, J. P.; Tanaka, E.; Frangioni, J. V.; Bawendi, M., Compact Cysteine-Coated CdSe(ZnCdS) Quantum Dots for in Vivo Applications. *J. Am. Chem. Soc.* **2007,** *129*, (47), 14530-14531.

19. Mattera, L.; Bhuckory, S.; Wegner, K. D.; Qiu, X.; Agnese, F.; Lincheneau, C.; Senden, T.; Djurado, D.; Charbonniere, L. J.; Hildebrandt, N.; Reiss, P., Compact quantum dot-antibody conjugates for FRET immunoassays with subnanomolar detection limits. *Nanoscale* **2016,** *8*, (21), 11275-83.

20. Bhuckory, S.; Mattera, L.; Wegner, K. D.; Qiu, X.; Wu, Y. T.; Charbonniere, L. J.; Reiss, P.; Hildebrandt, N., Direct conjugation of antibodies to the ZnS shell of quantum dots for FRET immunoassays with low picomolar detection limits. *Chem Commun* **2016,** *52*, (100), 14423-14425.

21. Stasiuk, G. J.; Tamang, S.; Imbert, D.; Poillot, C.; Giardiello, M.; Tisseyre, C.; Barbier, E. L.; Fries, P. H.; de Waard, M.; Reiss, P.; Mazzanti, M., Cell-Permeable Ln(III) Chelate-Functionalized InP Quantum Dots As Multimodal Imaging Agents. *ACS Nano* **2011,** *5*, (10), 8193-8201.

22. Stasiuk, G. J.; Tamang, S.; Imbert, D.; Gateau, C.; Reiss, P.; Fries, P.; Mazzanti, M., Optimizing the relaxivity of Gd(iii) complexes appended to InP/ZnS quantum dots by linker tuning. *Dalton Transactions* **2013,** *42*, (23), 8197-8200.

23. Molloy, J. K.; Lincheneau, C.; Karimdjy, M. M.; Agnese, F.; Mattera, L.; Gateau, C.; Reiss, P.; Imbert, D.; Mazzanti, M., Sensitisation of visible and NIR lanthanide emission by InPZnS quantum dots in bi-luminescent hybrids. *Chem. Commun.* **2016,** *52*, (24), 4577-4580.

24. Ambrosone, A.; Roopin, M.; Pelaz, B.; Abdelmonem, A. M.; Ackermann, L. M.; Mattera, L.; Allocca, M.; Tino, A.; Klapper, M.; Parak, W. J.; Levy, O.; Tortiglione, C., Dissecting common and divergent molecular pathways elicited by CdSe/ZnS quantum dots in freshwater and marine sentinel invertebrates. *Nanotoxicology* **2017,** *11*, (2), 289-303.

25. Ambrosone, A.; Mattera, L.; Marchesano, V.; Quarta, A.; Susha, A. S.; Tino, A.; Rogach, A. L.; Tortiglione, C., Mechanisms underlying toxicity induced by CdTe quantum dots determined in an invertebrate model organism. *Biomaterials* **2012,** *33*, (7), 1991-2000.

26. V.Marchesano, A. A., J. Bartelmess, F. Strisciante, A.Tino, L. Echegoyen, C.Tortiglione and S. Giordani Impact of Carbon Nano-Onions on Hydra vulgaris as a Model Organism for Nanoecotoxicology. *Nanomaterials* **2015,** *5*, (3), 1331- 1350.

27. Ambrosone, A.; Scotto di Vettimo, M. R.; Malvindi, M. A.; Roopin, M.; Levy, O.; Marchesano, V.; Pompa, P. P.; Tortiglione, C.; Tino, A., Impact of Amorphous SiO2 Nanoparticles on a Living Organism: Morphological, Behavioral, and Molecular Biology Implications. *Frontiers in bioengineering and biotechnology* **2014,** *2*, 37.

28. Tortiglione, C.; Quarta, A.; Malvindi, M. A.; Tino, A.; Pellegrino, T., Fluorescent nanocrystals reveal regulated portals of entry into and between the cells of Hydra. *PloS one* **2009,** *4*, (11), e7698.

29. Tortiglione, An ancient model organism to test in vivo novel functional nanocrystals In *Biomedical Engineering: from theory to application* Fazel-Rezai, R., Ed. InTech - Open Access Publisher: 2011; Vol. Biomedical Engineering: from theory to application pp 225-252.

30. Tino, A.; Ambrosone, A.; Mattera, L.; Marchesano, V.; Susha, A.; Rogach, A.; Tortiglione, C., A new in vivo model system to assess the toxicity of semiconductor nanocrystals. *International journal of biomaterials* **2011,** *2011*, 792854.

31. Ambrosone, A.; Marchesano, V.; Mazzarella, V.; Tortiglione, C., Nanotoxicology using the sea anemone Nematostella vectensis: from developmental toxicity to genotoxicology. *Nanotoxicology* **2014,** *8*, (5), 508-20.

32. Pellegrino, T.; Manna, L.; Kudera, S.; Liedl, T.; Koktysh, D.; Rogach, A. L.; Keller, S.; Radler, J.; Natile, G.; Parak, W. J., Hydrophobic nanocrystals coated with an amphiphilic polymer shell: A general route to water soluble nanocrystals. *Nano Lett* **2004,** *4*, (4), 703-707.

33. Malvindi, M. A.; Carbone, L.; Quarta, A.; Tino, A.; Manna, L.; Pellegrino, T.; Tortiglione, C., Rod-shaped nanocrystals elicit neuronal activity in vivo. *Small (Weinheim an der Bergstrasse, Germany)* **2008,** *4*, (10), 1747-55.

34. Lim, J.; Bae, W. K.; Lee, D.; Nam, M. K.; Jung, J.; Lee, C.; Char, K.; Lee, S., InP@ZnSeS, Core@Composition Gradient Shell Quantum Dots with Enhanced Stability. *Chem. Mater.* **2011,** *23*, (20), 4459-4463.

35. Loomis, W. F., and Lenhoff, H. M., Growth and sexual differentiation of Hydra in mass culture. . *J. Exp. Zool.* **1956,** *132*, 555-574.

36. Wilby, O. K.; Tesh, J. M., The Hydra assay as an early screen for teratogenic potential. *Toxicology in vitro : an international journal published in association with BIBRA* **1990,** *4*, (4-5), 582-3.

37. Bosch, T. C.; David, C. N., Growth regulation in Hydra: relationship between epithelial cell cycle length and growth rate. *Developmental biology* **1984,** *104*, (1), 161-71.

38. David, C. N., *A quantitative method for maceration of Hydra tissue*. Wilhelm Roux Arch. EntwMech. Org.: 1973; Vol. 171, p 259-268.

39. Livak, K. J.; Schmittgen, T. D., Analysis of relative gene expression data using real-time quantitative PCR and the 2(-Delta Delta C(T)) Method. *Methods (San Diego, Calif* **2001,** *25*, (4), 402-8.

40. Marchesano, V.; Hernandez, Y.; Salvenmoser, W.; Ambrosone, A.; Tino, A.; Hobmayer, B.; M de la Fuente, J.; Tortiglione, C., Imaging inward and outward trafficking of gold nanoparticles in whole animals. *ACS nano* **2013,** *7*, (3), 2431-2442.

41. Ambrosone, A.; Tortiglione, C., Methodological approaches for nanotoxicology using cnidarian models. *Toxicology mechanisms and methods* **2013,** *23*, (3), 207-216.

42. Ambrosone, A., Marchesano, V., Mattera, L., Tino, A., Tortiglione, C., Bridging the fields of nanoscience and toxicology: nanoparticle impact on biological models. In *Colloidal Quantum Dots/Nanocrystals for Biomedical Applications VI*, Parak, W. J. Y. K. O. M., Ed. SPIE, Bellingham, WA: Washington, USA, 2011; Vol. 7909.

43. Elmore, S., Apoptosis: a review of programmed cell death. *Toxicologic pathology* **2007,** *35*, (4), 495-516.

44. David, C. N.; Schmidt, N.; Schade, M.; Pauly, B.; Alexandrova, O.; Bottger, A., Hydra and the evolution of apoptosis. *Integrative and comparative biology* **2005,** *45*, (4), 631-8.

45. Galliot, B.; Chera, S., The Hydra model: disclosing an apoptosis-driven generator of Wnt-based regeneration. *Trends in cell biology* **2010,** *20*, (9), 514-23.

46. Moros, M.; Ambrosone, A.; Stepien, G.; Fabozzi, F.; Marchesano, V.; Castaldi, A.; Tino, A.; de la Fuente, J. M.; Tortiglione, C., Deciphering intracellular events triggered by mild magnetic hyperthermia in vitro and in vivo. *Nanomedicine* **2015,** *10*, (14), 2167-83.

47. Cikala, M.; Wilm, B.; Hobmayer, E.; Bottger, A.; David, C. N., Identification of caspases and apoptosis in the simple metazoan Hydra. *Current biology : CB* **1999,** *9*, (17), 959-62.

48. Lasi, M.; David, C. N.; Bottger, A., Apoptosis in pre-Bilaterians: Hydra as a model. *Apoptosis : an international journal on programmed cell death* **2010,** *15*, (3), 269-78.

49. Tino, A.; Ambrosone, A.; Marchesano, V.; Tortiglione, C., Molecular Bases of Nanotoxicology. In *Bio- and Bioinspired Nanomaterials*, Wiley-VCH Verlag GmbH & Co. KG: Weinheim, Germany, 2014.

50. Chapman, J. A.; Kirkness, E. F.; Simakov, O.; Hampson, S. E.; Mitros, T.; Weinmaier, T.; Rattei, T.; Balasubramanian, P. G.; Borman, J.; Busam, D.; Disbennett, K.; Pfannkoch, C.; Sumin, N.; Sutton, G. G.; Viswanathan, L. D.; Walenz, B.; Goodstein, D. M.; Hellsten, U.; Kawashima, T.; Prochnik, S. E.; Putnam, N. H.; Shu, S.; Blumberg, B.; Dana, C. E.; Gee, L.; Kibler, D. F.; Law, L.; Lindgens, D.; Martinez, D. E.; Peng, J.; Wigge, P. A.; Bertulat, B.; Guder, C.; Nakamura, Y.; Ozbek, S.; Watanabe, H.; Khalturin, K.; Hemmrich, G.; Franke, A.; Augustin, R.; Fraune, S.; Hayakawa, E.; Hayakawa, S.; Hirose, M.; Hwang, J. S.; Ikeo, K.; Nishimiya-Fujisawa, C.; Ogura, A.; Takahashi, T.; Steinmetz, P. R.; Zhang, X.; Aufschnaiter, R.; Eder, M. K.; Gorny, A. K.; Salvenmoser, W.; Heimberg, A. M.; Wheeler, B. M.; Peterson, K. J.; Bottger, A.; Tischler, P.; Wolf, A.; Gojobori, T.; Remington, K. A.; Strausberg, R. L.; Venter, J. C.; Technau, U.; Hobmayer, B.; Bosch, T. C.; Holstein, T. W.; Fujisawa, T.; Bode, H. R.; David, C. N.; Rokhsar, D. S.; Steele, R. E., The dynamic genome of Hydra. *Nature* **2010,** *464*, (7288), 592-6.

51. Campion, S.; Aubrecht, J.; Boekelheide, K.; Brewster, D. W.; Vaidya, V. S.; Anderson, L.; Burt, D.; Dere, E.; Hwang, K.; Pacheco, S.; Saikumar, J.; Schomaker, S.; Sigman, M.; Goodsaid, F., The current status of biomarkers for predicting toxicity. *Expert opinion on drug metabolism & toxicology* **2013,** *9*, (11), 1391-408.

52. Tuszynski, G. P.; Gasic, T. B.; Gasic, G. J., Isolation and characterization of antistasin. An inhibitor of metastasis and coagulation. *The Journal of biological chemistry* **1987,** *262*, (20), 9718-23.

53. Holstein, T. W.; Mala, C.; Kurz, E.; Bauer, K.; Greber, M.; David, C. N., The primitive metazoan Hydra expresses antistasin, a serine protease inhibitor of vertebrate blood coagulation:

774 cDNA cloning, cellular localisation and developmental regulation. *FEBS Lett* **1992,** *309*, (3), 288-
775 92.

776 54. Mondal M.; Khanra S.; Tiwari O.N.; Gayen K.; G.N., H., Role of carbonic anhydrase on the
777 way to biological carbon capture through microalgae—A mini review. *Environmental progress and*
778 *sustainable energy* **2016,** *35*, 1605-1615.

779 55. Lionetto, M. G.; Caricato, R.; Giordano, M. E.; Erroi, E.; Schettino, T., Carbonic anhydrase
780 as pollution biomarker: an ancient enzyme with a new use. *International journal of environmental*
781 *research and public health* **2012,** *9*, (11), 3965-77.

782 56. Lionetto, M. G.; Caricato, R.; Giordano, M. E.; Schettino, T., The Complex Relationship
783 between Metals and Carbonic Anhydrase: New Insights and Perspectives. *International journal of*
784 *molecular sciences* **2016,** *17*, (1), 127-141.

785 57. Wang, B.; Liu, C. Q.; Wu, Y., Effect of heavy metals on the activity of external carbonic
786 anhydrase of microalga Chlamydomonas reinhardtii and microalgae from karst lakes. *Bulletin of*
787 *environmental contamination and toxicology* **2005,** *74*, (2), 227-33.

788 58. Morel F.M.M., R. J. R., Roberts S.B., Chamberlain C.P., Lee J.G., Yee D., Zinc and carbon
789 co-limitation of marine phytoplankton. *Nature* **1994,** *369*, 740-742.

790 59. Lee J.G., R. S. B., Morel F.M.M. , Cadmium: A nutrient for the marine diatom Thalassiosira
791 weissflogii. *Limnology and oceanography* **1995,** *40*, 1050-1063.

792

793